Yu.F. Zhukovskii[1], D. Bocharov[2,3], D. Gryaznov[1], and E.A. Kotomin[1]

First principles simulations on surface properties and oxidation of uranium mononitride

[1]Institute of Solid State Physics, Kengaraga 8, LV- 1063, [2]Faculty of Computing, University of Latvia, Raina blvd. 19, LV-1586, [3]Faculty of Physics and Mathematics, University of Latvia, Zellu 8, LV-1002 e-mail of presenting author: quantzh@latnet.lv

ESF EIROPAS SOCIĀLAIS FONDS
EIROPAS SAVIENĪBA
IEGULDĪJUMS TAVĀ NĀKOTNĒ

Motivation

The uranium mononitride (UN), which possesses a rock-salt (NaCl) structure and metallic nature, is an advanced material for the non-oxide nuclear fuel considered as a promising candidate to be used in Generation-IV nuclear reactors. However, UN samples synthesized for reactors contain considerable amount of O impurities, which greatly affect fuel properties. Therefore, it is necessary to understand the mechanism of both oxygen adsorption and further oxidation of uranium mononitride.

Computational method and model

We have performed detailed study of UN surfaces and their reactivity using slab model [1-5].To simplify modeling of the oxygen interaction with UN surface, we study mainly the (001) surface since according to Tasker analysis [6] it has the lowest surface energy. Nevertheless, synthesized specimens of polycrystalline UN contains particles with differently oriented crystallographic facets [7]. Therefore, to increase validity of our results, we have additionally performed (110) surface calculations. We chose (110) surface orientation for additional calculations since alternative low-indiced (111) surface contains charged planes and its calculation requires artificial approaches. We simulated reconstruction of perfect and defective UN(110) surface as well as atomic oxygen adsorption, formation of N vacancies and oxygen incorporation into them.

For calculations we employ the DFT plane-wave computational package *VASP 4.6* [8], using ultra-soft pseudopotentials combined with the PAW method. We use the Perdew-Wang-91 GGA non-local exchange-correlation functional [9] and the scalar relativistic PAW pseudopotentials representing the core electrons of U (with $6s^2 6p^6 6d^2 5f^2 7s^2$ valence shell), N ($2s^2 2p^3$) and O ($2s^2 2p^4$) atoms (containing 14, 5 and 6 valence electrons, respectively). The cut-off energy is chosen to be 520 eV. We use the Monkhorst-Pack scheme [10] for 4x4x1 and 8x8x1 *k*-point meshes in the Brillouin zone (BZ).

For the UN(001) and (110) substrates, we use 3D slab model consisting of 5-11 atomic layers with primitive cell as well as 2x2 and 3x3 supercels (Fig. 1). The 2D atomic slabs are separated by a vacuum gaps of ~40 Å (Fig. 2).

The lattice constant of UN slabs is fixed at 4.87 Å, taken from the lattice relaxation of UN bulk [5]. In all the calculations, we perform the structural optimization within the supercell of fixed linear dimensions. The total spin magnetic moment is also relaxed in all the calculations on the ferromagnetic spin distributions within the uranium sub-lattice.

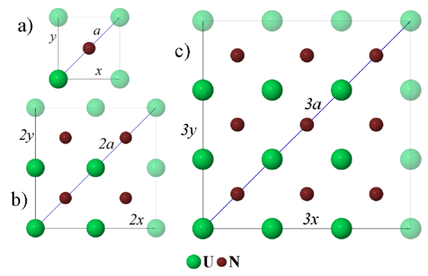

Fig. 1. Atop views of primitive cell (a) as well as 2×2 (b) and 3×3 (c) supercells upon UN (001) surface.

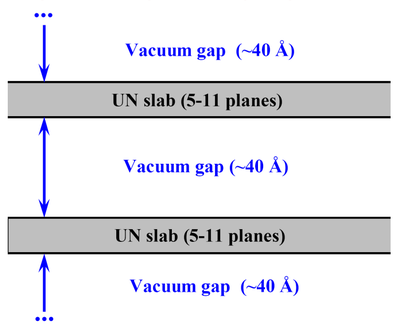

Fig. 2. Cross-section of 3D UN slabs.

Molecular and atomic O adsorption on UN surface

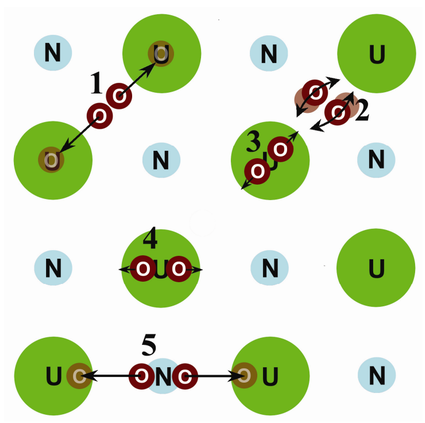

Fig. 3. Schematic view of five different horizontal configurations for the O_2 molecule adsorption on UN surface: 1) atop the hollow site oriented towards the nearest Usurf atoms, 2) atop the hollow site oriented towards the nearest N_{surf} atoms, 3) atop the U_{surf} atoms oriented towards the next-nearest surface U_{surf} atoms, 4) atop the U_{surf} atoms oriented towards the nearest N_{surf} atoms, 5) atop the N_{surf} atoms oriented towards the nearest U_{surf} atoms.

We show that spontaneous dissociation of molecule can occur when O_2 is located either atop the hollow site (1) or atop the N_{surf} atom (5) (Fig. 3).

$$E_{bind} = \frac{1}{2}\left(E^{\mathrm{UN}} + 2E^{\mathrm{O_{triplet}}} - E^{\mathrm{O/UN}}\right)$$

O adatom forms a strong chemical bond with the U_{surf} atom beneath which can be considered as one-center surface complex. In the case of O adatom positioned atop the N_{surf} atom, this complex is rather multi-center which involves 4 adjacent U_{surf} atoms.

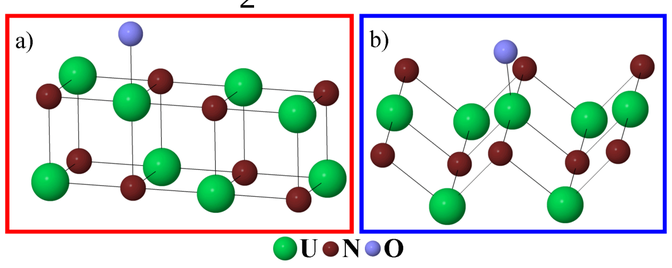

Fig. 4. 2-layer models of oxygen adsorption atop surface U atom on UN (001) (a) and (110) (b) surface

For both surfaces, oxygen binding energy with U atom is larger as compared to that with N atom (~1.9 eV for (001) and ~2.1-2.2 eV for (110) surface, Table 1).

Oxygen binding energies on (110) surface are ~0.1-0.4 eV larger as compared to (001) surface.

Higher E_{bind} values for (110) surface can be explained by larger distances between surface adatoms upon (110) surface resulting in decreased interactions between adsorbed oxygen and all other atoms, excluding underlying U or N atom.

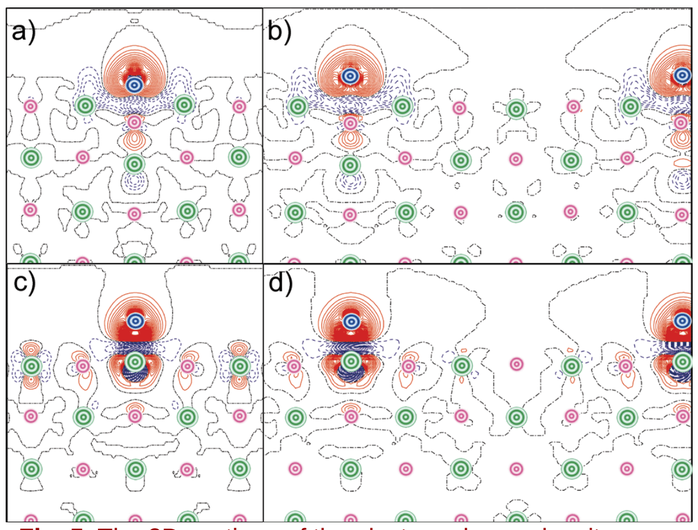

Fig. 5. The 2D sections of the electron charge density re-distributions $\Delta\rho(\mathbf{r})$ for O atoms adsorbed atop (*i*) N_{surf} atom for 2×2 (a) and 3×3 (b) supercells as well as (*ii*) U_{surf} atom for 2×2 (c) and 3×3 (d) supercells upon the seven-layer UN(001) slab.

Table 1. The calculated binding energies (E_{bind}, eV) for oxygen adsorption atop UN (001) and (110) surfaces.

		Atop U	Atop N
Number of layers and supercell size		Binding energy, eV	Binding energy, eV
(001)	7, 2×2	7.51	5.58
	7, 3×3	7.57	5.65
(110)	7, 2×2	7.90	5.73
	7, 3×3	7.91	5.99

O atom incorporation into defective UN(001) slab

According to our calculations, O atom adsorbed atop the U_{surf} atom in the proximity of the surface N vacancy can be captured by the latter when overcoming a low energy barrier (~0.5-1 eV).

$$E_I = \frac{1}{2}\left(E^{\mathrm{UN(O\_}inc\mathrm{)}} - E^{\mathrm{UN(N\_vac)}} - 2E^{O}\right) \quad E_S = E_I + E_{form}$$

Table 2. Incorporation (E_I) and solution (E_S) energies, average spin magnetic moments of U atoms and effective charge on O atoms for oxygen incorporated into N vacancy on UN (001) [7] and (110) surfaces. The reference states for calculations on the incorporation and solution energies are the chemical potentials of O and N calculated for O_2 and N_2 molecules, respectively (2×2 and 3×3 supercells).

Number of layers	E_I (eV)	E_S (eV)	μ_{av}^{U} (μ_B)	q_{eff} (e^-)	E_I (eV)	E_S (eV)	μ_{av}^{U} (μ_B)	q_{eff} (e^-)
	(001) surface				(110) surface			
5, 2×2	-6.173	-2.473	1.647	-1.36	-5.853	-2.778	1.736	-1.27
7, 2×2	-6.181	-2.476	1.495	-1.36	-5.822	-2.794	1.516	-1.29
9, 2×2	-6.186	-2.479	1.412	-1.36	-5.820	-2.784	1.472	-1.29
11, 2×2	-6.195	-2.483	1.365	-1.35	-5.817	-2.791	1.416	-1.29
7, 3×3	-6.126	-2.480	1.463	-1.36	-5.748	-2.783	1.471	-1.28

Fig. 6. 2-layer models of oxygen incorporation into surface N vacancy on UN (001) (a) and (110) (b) surface

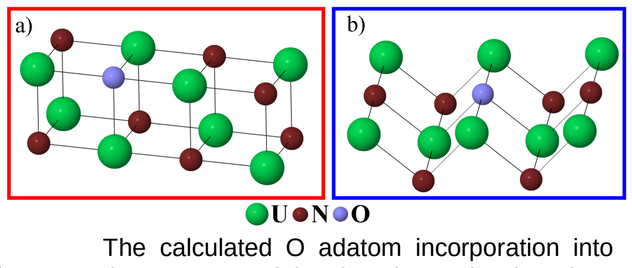

The calculated O adatom incorporation into the N vacancy (Fig. 6) at the UN(001) surface has been found to be energetically favorable since both values of E_I and E_S are strictly negative (Table 2). This is in favor of both creation of the N vacancy and adsorption of the O atom from air. (In contrary, in the case of U vacancies, the values of E_I calculated for the surface and central layers have been found to be close to zero).

Perfect UN surface calculations

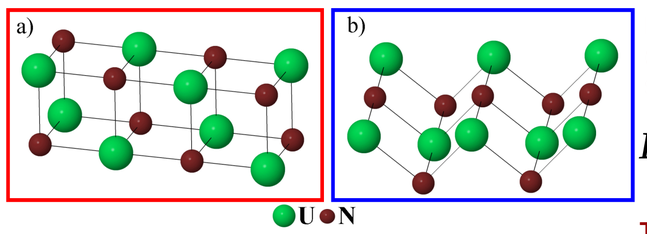

Fig. 7. 2-layer models of UN (001) (a) and UN (110) (b) surfaces.

$$E_{surf}(n) = \frac{1}{2S}(E_n - nE_b)$$

Table 3. Surface energies E_{surf} (J·m^{-2}) and averaged magnetic moments (in μ_B) of U atom for the defectless UN (001) [5, 6] and UN(110) surfaces. In spin-frozen calculations, μ was chosen to be 1 μ_B.

Number of layers	E_{surf} (J·m^{-2}) spin-frozen slab (001)	E_{surf} (J·m^{-2}) spin-relaxed slab (001)	μ_{av}(μ_B) (001)	E_{surf} (J·m^{-2}) spin-relaxed slab (110)	μ_{av}(μ_B) (110)
5	1.69	1.44	1.57	1.977	1.645
7	1.70	1.37	1.44	1.928	1.464
9	1.70	1.29	1.37	1.878	1.417
11	1.69	1.22	1.33	1.830	1.385

Table 4. Atomic Bader charges for the defectless spin-relaxed UN (001) and (110) surfaces.

	Number of UN (001) slab atomic layers				Number of UN (110) slab atomic layers			
Atom	5	7	9	11	5	7	9	11
Surface U	1.68	1.74	1.68	1.72	1.46	1.48	1.49	1.48
Sub-surface U	1.67	1.63	1.63	1.67	1.88	1.85	1.83	1.84
U in central (mirror) plane	1.69	1.72	1.65	1.66	1.60	1.74	1.64	1.70
Surface N	-1.65	-1.67	-1.67	-1.68	-1.55	-1.55	-1.55	-1.55
Sub-surface N	-1.68	-1.70	-1.70	-1.67	-1.75	-1.73	-1.75	-1.73
N in central (mirror) plane	-1.74	-1.65	-1.65	- 1.63	- 1.70	-1.71	-1.75	-1.74

Depending on slab thickness, the surface energies are ~0.5-0.7 J·m^{-2} larger for UN(110) surface (Table 3). It means that the UN(001) surface is energetically more favorable.

It is also interesting to analyze q_{eff} values for atoms across the slab as a function of the number of layers in a slab (Table 4). First, these q_{eff} show considerable covalent bonding both on the surface (*e.g.*, sub-surface) and on the central plane since the values. Second, due to different reconstruction mechanisms of UN(001) and UN(110) surfaces, the atomic charges are different too: ionicity of bonds at (001) surface is higher, thus leading to certain difference in surface properties.

N vacancies on (001) and (110) surface

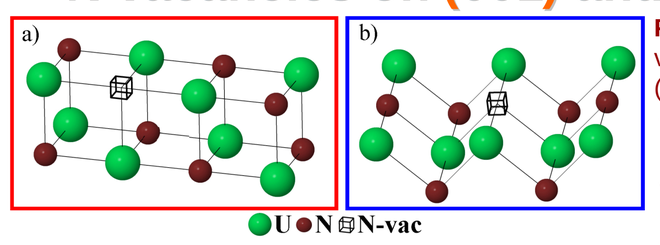

Fig. 8. 2-layer models of N vacancy on UN (001) (a) and (110) (b) surface

Table 5. Nitrogen vacancy formation energies (in eV) as well as averaged magnetic moment μ_{av} of U atom evaluated for UN (001) and (110) surfaces.

Number of layers and supercell size	N vacancy E_{form} on (001) surface	μ_{av}(μ_B) (001)	N vacancy E_{form} on (110) surface	μ_{av}(μ_B) (110)
5, 2×2	3.700	1.702	3.075	1.818
7, 2×2	3.706	1.548	3.028	1.585
9, 2×2	3.708	1.452	3.036	1.512
11, 2×2	3.712	1.392	3.026	1.453
7, 3×3	3.646	1.487	2.966	1.498

Basic tendencies remain similar for vacancies on (001) and (110) surface (Table 5). Averaged magnetic moment μ_{av} decreases as a function of a number of layers in the slab for both surfaces.

On the other hand, vacancy formation energies are by ~0.7 eV smaller for UN(110) surface. This distinction is easy explainable due to a larger friability of the (110) surface as compared to the (001) surface.

$$E_{form}^{\mathrm{N(U)}vac} = \frac{1}{2}\left(E^{\mathrm{UN(N\_vac)}} + 2E^{\mathrm{N}} - E^{\mathrm{UN}}\right)$$

Summary

q The PAW method is used to analyze basic UN bulk and surface properties, point defects behavior on UN surface as well as oxygen interaction with UN surface.

q Comparison of UN (001) and UN (110) surfaces shows that the former is energetically more favorable. This fact allow us to perform both calculations on defectless UN surface and oxygen adsorbtion upon the (001) surface mainly.

q The formation energies for U and N vacancies indicate a clear trend for segregation of vacancies towards the surface (and probably, grain boundaries).

q Results obtained for interaction of O atoms and O_2 molecules with UN surfaces demonstrate a strong chemisorption, typical for metallic adsorbents. The possibility for spontaneous dissociation of the adsorbed oxygen molecules upon the perfect UN (001) surface, analogously to the O_2 dissociation on metallic surfaces, has been demonstrated.

q In the case of defective substrate, presence of the surface nitrogen vacancy closest to the surface U atom (U_{surf}) results in a low-barrier incorporation of migrating O adatom from position atop U_{surf} towards this vacancy, which can be considered as a trap.

q The following stages for reactivity of oxygen positioned atop the UN surface could be suggested: (*i*) chemisorption of molecular oxygen, (*ii*) spontaneous breaking of the O_2 chemical bond after molecular adsorption, (*iii*) location of the two newly formed O adatoms atop the adjacent surface U atoms, (*iv*) high mobility of O_{ads} atoms along the surface, (*v*) low-barrier incorporation of oxygen adatoms from the positions atop U_{surf} atoms into the nearest N vacancies, *(vi)* stabilization of O_{ads} atom inside N_{surf} vacancy, (*vii*) incorporation of O atoms in existing subsurface N vacancies as a result of inter-lattice diffusion.

q This can explain an easy UN oxidation observed in air.

Acknowledgements

This study was supported by the ERAF grant 2DP/2.1.1.2.0/10/APIA/VIAA/010, ESF project No. 2009/0216/1DP/1.1.1.2.0/09/APIA/VIAA/044 and European Commission FP7 project *F-BRIDGE*. The authors thank R.A. Evarestov, S. Piskunov, P. Nazarov, J. Chepkasova, J. Timoshenko, A. Kuzmin, P. Van Uffelen and V. Kashcheyevs for a numerous fruitful discussions. The technical assistance of A. Gopejenko and A. Gusev was the most valuable.

References

[1]. R.A. Evarestov, A.V. Bandura, M.V. Losev, E.A. Kotomin, Yu.F. Zhukovskii, and D. Bocharov, J. *Comput. Chem.* 29 (2008) 2079.
[2]. Yu.F. Zhukovskii, D. Bocharov, and E.A. Kotomin, J. Nucl. Mater., 393 (2009) 504.
[3]. Yu.F. Zhukovskii, D. Bocharov, E.A. Kotomin, R.A. Evarestov, and A.V. Bandura, Surf. Sci., 603 (2009) 50.
[4]. D. Bocharov, D. Gryaznov, Yu.F. Zhukovskii, and E.A. Kotomin, *Surf. Sci.*, 605 (2011) 396.
[5]. D. Bocharov, D. Gryaznov, Yu.F. Zhukovskii, E.A. Kotomin, *J. Nucl. Mater.*, 416 (2011) 200.
[6] P.W. Tasker, *J. Phys. C: Solid State Phys.*, 12 **(**1979) 4977.
[7] G.W. Chinthaka Silva, Ch.B. Yeamans, L. Ma, G.S. Cerefice, K.R. Czerwinski, and A.P. Sattelberger, *Chem. Mat.*, 20 (2008) 3076.
[8]. G. Kresse and J. Hafner, *VASP the Guide* (University of Vienna, 2007).
[9]. J.P. Perdew and Y. Wang, *Phys. Rev. B* 45 (1992) 13244.
[10]. H.J. Monkhorst and J.D. Pack, *Phys. Rev. B*, **13** (1976) 5188.